Viscosity, Yield Stress, Slip, and Natural Convection of HSPAN Gel–Water Dispersions

RICHARD A. HARDIN and LOUIS C. BURMEISTER*

Department of Mechanical Engineering, University of Kansas, Lawrence, Kansas 66045-2234

SYNOPSIS

Three hydrolyzed-starch–polyacrylonitrile (HSPAN) copolymer materials tested as gel–water dispersions in a Brookfield rotating spindle viscometer exhibited velocity slip at solid boundaries and a yield stress. Dispersions with 0.5% HSPAN concentrations were about 20,000 times more viscous than water when the shear stress surpassed the yield stress and viscous power-law flow ensued. The apparent viscosity of an HSPAN gel–water dispersion was reduced by nearly an order of magnitude when tap water was substituted for deionized water. The apparent viscosity of the HSPAN gel–water dispersions decreased by about 30% after the fluid was continuously maintained at a temperature of 80°C for 1 week, and by an order of magnitude or more after 3 weeks under those conditions. In natural convection tests, the yield stress enabled an HSPAN gel–water dispersion to withstand greater temperature differences across a horizontal layer before inception of natural convection than a fluid without one. © 1993 John Wiley & Sons, Inc.

INTRODUCTION

A copolymer made from starch was developed in the early 1970s at the U.S. Department of Agriculture Northern Regional Research Laboratory in Peoria, Illinois. As described by Weaver et al.[1] and Otey and Doane,[2] it can absorb large amounts of water and is commercially available in flake or powder form. Because of its absorptive power, up to 800 times its weight of distilled water, it is sometimes referred to as a slurper although it is more generally known as an HSPAN (hydrolyzed-starch–polyacrylonitrile) material.

As reported by Stannett et al.,[3] dispersions of HSPAN gel in water can be 20,000 times more viscous than water. The high viscosities were described by Taylor and Bagley[4] as due to the formation of a system of swollen, deformable gel particles that are closely packed. They state that neither the minor amount of copolymer in solution nor the size of the gel particles exerts a large influence on rheological properties. When either the ionic strength of the aqueous medium is increased or the swollen gel is diluted to the point that the solvent is in excess, the gel particles are no longer tightly packed, and the viscosity of the system sharply drops. The criteria for the condition where gel particles are closely packed and no excess solvent is present were reported by Taylor and Bagley.[5] In contrast to the high viscosities of aqueous dispersions of HSPAN gel, the viscosities of HSPAN solutions (obtained by degrading HSPAN gel with excessive mechanical shearing such as can be produced by ultrasound) are low and almost Newtonian, according to Bagley and Taylor.[6]

Measurements of apparent viscosities of HSPAN gel–water dispersions were reported by Gugliemelli et al.[7] The apparent viscosity of 1% (by mass of HSPAN gel) dispersions in distilled water measured at room temperature with a Brookfield Synco-lectric LVT viscometer with a no. 4 spindle at 30 rpm had a peak value of about 20,000 cP (1 cP = 10^{-3} N s/m^2), decreasing nearly linearly to about 2000 cP as the dispersion percentage decreased to 0.063% and decreasing by about a factor of 3 as the pH of the dispersion was varied by a factor of 2 from the value of 8.5. Although not stated to be a power-law fluid, the apparent viscosity was shown to vary with strain rate in a manner suggestive of that behavior. The apparent viscosities decreased by a factor of 2

* To whom correspondence should be addressed.

Journal of Applied Polymer Science, Vol. 48, 625–637 (1993)
 CCC 0021-8995/93/040625-13

when 1% KCl salt was added to the dispersion, and diminished to 1,100 cP at 8% KCl. The dispersions were reported to be stable after 0.5 h at 100°C, at which temperature the apparent viscosities were only slightly reduced.

Later, Weaver et al.[8] reported measurements of the variation of the ratio of apparent viscosity to gel concentration vs. the concentration, made in the same manner. At concentrations above 0.1%, the ratio was nearly constant but dependent upon the nature of the HSPAN gel tested.

Because some HSPAN gel–water dispersions are somewhat transparent, their use in a viscosity stabilized solar pond has been proposed. This apparently new application requires measurements of the viscosities of HSPAN gel–water dispersions over a range of shearing rates both before and after extended times above room temperatures that are more detailed than those previously reported. Such measurements, their correlation, and the methods by which they were made for several commercially available HSPAN materials are described in the following.

APPARATUS AND PROCEDURE

A Brookfield LVTD rotating-spindle viscometer, providing eight rotational speeds (0.3, 0.6, 1.5, 3.0, 6.0, 12.0, 30.0, and 60.0 rpm) was used. Cylindrical spindles of two types, (no. 1, 6.5 cm long and 1.88 cm diameter, and no. 4, 3.58 cm long and 0.32 cm diameter) were used for measurements from which yield stress and slip coefficient values were derived, although a disk-shaped spindle (no. 18) was also employed in exploratory measurements. Measurements of viscosity were made with the fluid in an 800 mL beaker of 10.4 cm diameter filled 10.2 cm deep.

The dry HSPAN material in the form of powder or small flakes obtained from three commercial sources used in this study was: (1) Super-Sorb and Ag Sorbent Flakes (Super Absorbent Co., Lumberton, NC), (2) Sta-Wet (Polysorb Inc., Smelterville, ID), and (3) Water Lock A-200 and G-400 (Grain Processing Corp., Muscatine, IA).

Dispersions of HSPAN gel in water were prepared by slowly adding the dry material to continuously stirred water. Preparations in both distilled and tap water were made in this manner. Batches of 0.01–1% by mass of HSPAN material to water so prepared were allowed to set for at least 24 h before viscosity measurements were undertaken, during which time the containers were covered to inhibit evaporation of water. Viscometer readings were observed gradually to increase for setting times shorter than 24 h, suggesting that a gel structure was either established or reestablished with 24 h.

During a viscosity measurement, the torque output of the Brookfield viscometer was continuously recorded on a strip-chart recorder as illustrated by Van Wazer et al.[9] A substantial amount of time, amounting to 4–10 h in some cases, was required for the readings to stabilize at a nearly constant value. A mechanical structure appeared to repeatedly build up and break down as evidenced by fluctuation about the quasisteady state.

Viscosity measurements were also made after maintaining the HSPAN gel–water dispersion at temperatures near 80°C for a period of up to 3 weeks. The time at extended elevated temperature was achieved in two ways. In the first way, an insulated and covered beaker filled with an HSPAN gel–water dispersion was placed atop a hot plate maintained at a steady elevated temperature of about 80°C. The character of the dispersion was visually determined at intervals, and, after several weeks, the viscosity was measured at room temperature and compared with the value it had before heating.

In the second way, the HSPAN gel–water dispersion was placed into a natural convection cell, shown in Figure 1, constructed for the purpose of determining the temperature difference across a horizontal layer of HSPAN gel–water dispersion, heated at the bottom and cooled at the top, required to initiate natural convection. The cell consisted of a flexible fluroplastic immersion heater below a 0.32 × 24.8 × 24.8 cm aluminum plate at the bottom of a square container with a cooled aluminum plate at the top. Due to the 110°C temperature limitation of the heater, the bottom temperature of the contained fluid could not exceed 80°C, which was achieved with a maximum power input of 60 W. The container was made of styrofoam insulation limited to a maximum temperature of 74°C for continuous operation. Three layers of styrofoam board were cemented and sealed along the side and bottom edges to provide a total wall thickness of 15.24 cm. The top of the cell had a removable water-cooled aluminum cover insulated on top. Electrical energy was supplied to the heater at a rate determined by measuring the voltage difference, controlled by a Variac after first passing through a voltage regulator to minimize the effect of fluctuations in the line voltage, imposed across the heater and the current that flowed through the heater; the product of voltage drop and current equaled the heat flow. The heat loss QL through the

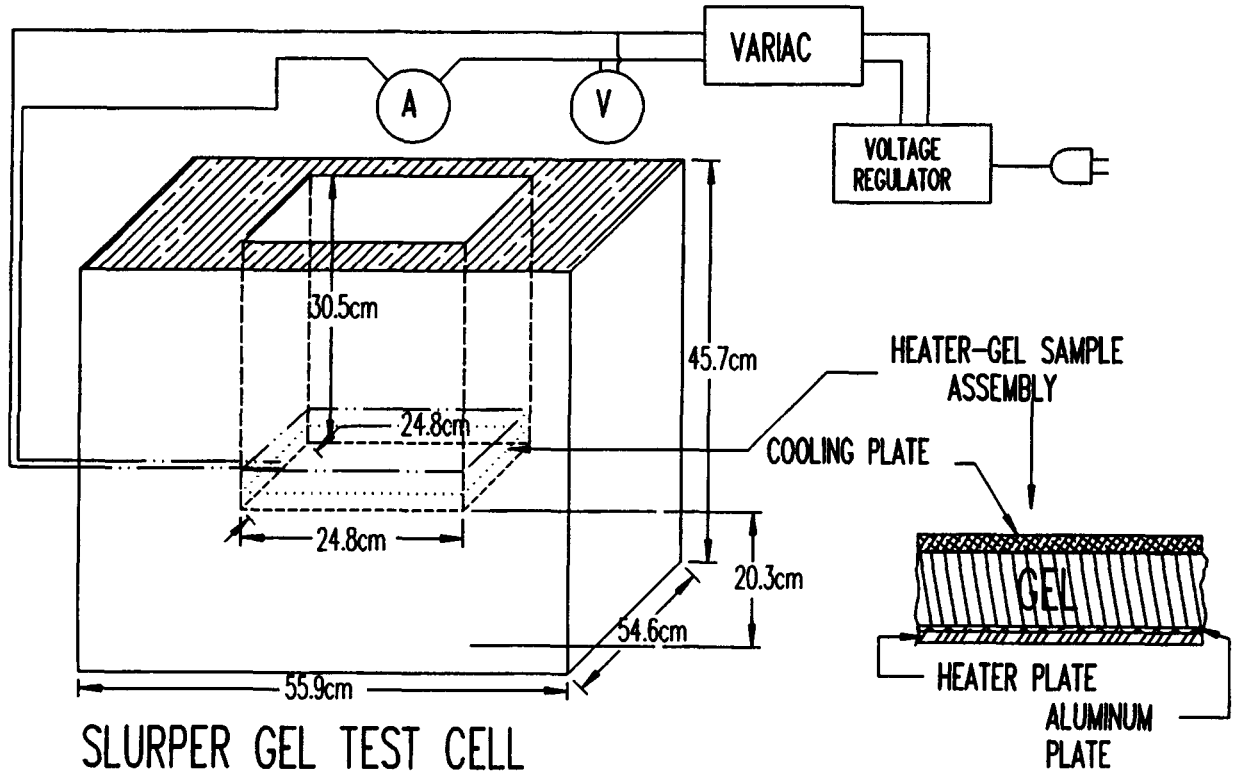

Figure 1 Natural convection test cell and apparatus.

bottom and sides of the styrofoam was estimated from the relationship

$$QL = KL(T_{av} - T_r)$$

where $T_{av} = ((T_{top} + T_{bo})/2 + T_{uh})/2$. Measurement of the energy supplied to the natural convection cell with a thick styrofoam cover replacing the water-cooled aluminum plate at the top, along with measurement of the temperature in the interior of the cell and the room temperature, gave the loss coefficient KL to be 0.0607 W/°C. The heat loss QL was typically about 10% of the input to the electrical heater. This heat loss was subtracted from the heat supplied to the heater to obtain the heat flow rate up through the HSPAN gel–water dispersion. Type K thermocouples were emplaced in one position below the immersion heater, in three atop the bottom aluminum plate, and in three on the bottom of the upper aluminum plate. The vertical temperature difference across the horizontal fluid layer was determined as the difference of the average of the three temperatures at the top and at the bottom of the fluid. A digital thermometer accurate to 0.1°C was used to convert the thermocouple output voltage to temperature.

The 3.8–7.6 cm thickness of the horizontal layer of HSPAN gel–water dispersion was selected on the basis of preliminary viscosity measurements fitted with a power-law model and a corresponding power-law criterion reported in the survey of Shenoy[10] for the onset of natural convection in the range of temperature differences imposed in these tests. For this range of thicknesses it was expected that the critical Rayleigh number for initiation of natural convection would be independent of the other cell dimensions, according to the studies for a Newtonian fluid by Catton[11,12] for conducting walls, Catton[13] for insulating walls, and Churchill[14] for both rectangular and circular cross-section enclosures heated from below.

NATURAL CONVECTION TEST CELL MEASUREMENTS

The natural convection test cell was employed to determine the temperature difference that could be imposed across a horizontal layer of HSPAN material–water dispersion before inception of natural convection. To establish the accuracy of the apparatus, tests were first performed with a 1.27-cm-thick

layer of glycerin, a Newtonian fluid whose properties are known. The results were in good agreement with the correlation of Hollands et al.[15]:

$$Nu = 1 + 1.44(1 - 1708/Ra)^* + [(Ra/5{,}830)^{1/3} - 1]^*$$

in which the $(\ )^*$ notation signifies that the quantity is to be taken as zero if the argument is negative. As expected, natural convection had its inception at Ra = 1708.

Tests with the T-25-A200 HSPAN material in a 3.81 cm thick layer gave the results shown in Figure 2. The dates on which the measurements were made are shown there. The Nusselt number value of 1.2 in the absence of natural convection was expected to be 1.0, a discrepancy that appears to be due to a shift in the convection cell heat loss that may have been caused by a gradually developing leak. Even with consideration of this peculiarity, the final two data points, those for 1/31–2/1/90, show a marked increase in Nusselt number that is best explained by the occurrence of natural convection. The bottom plate temperature fluctuated noticeably, too, strengthening the suggestion that natural convection had occurred for the abberant data points. All fluid properties other than viscosity were taken to be those of water, consistent with the findings of Makino et al.[16]

Apparently, the fresh HSPAN–water dispersion inhibited natural convection at temperature differences across a horizontal fluid layer that would have caused it to occur in either a Newtonian or a power-law fluid. The temperature difference and the fluid layer thickness were sufficiently large, certainly, for natural convection to have occurred.

Additional tests in the natural convection test cell with other HSPAN materials in both distilled and tap water had essentially the same results. In some of these additional tests, extra insulation was added to reduce possible unaccounted-for heat losses, thermocouples were inserted into the midregion of the fluid to ascertain whether or not the temperature distribution in the fluid was linear, as is characteristic of the absence of convection, and plexiglass viewing ports were installed to enable visual detection of fluid motion.

APPARENT VISCOSITY MEASUREMENTS

A notation to identify HSPAN gel–water dispersion viscometer data was devised. Four identifiers are

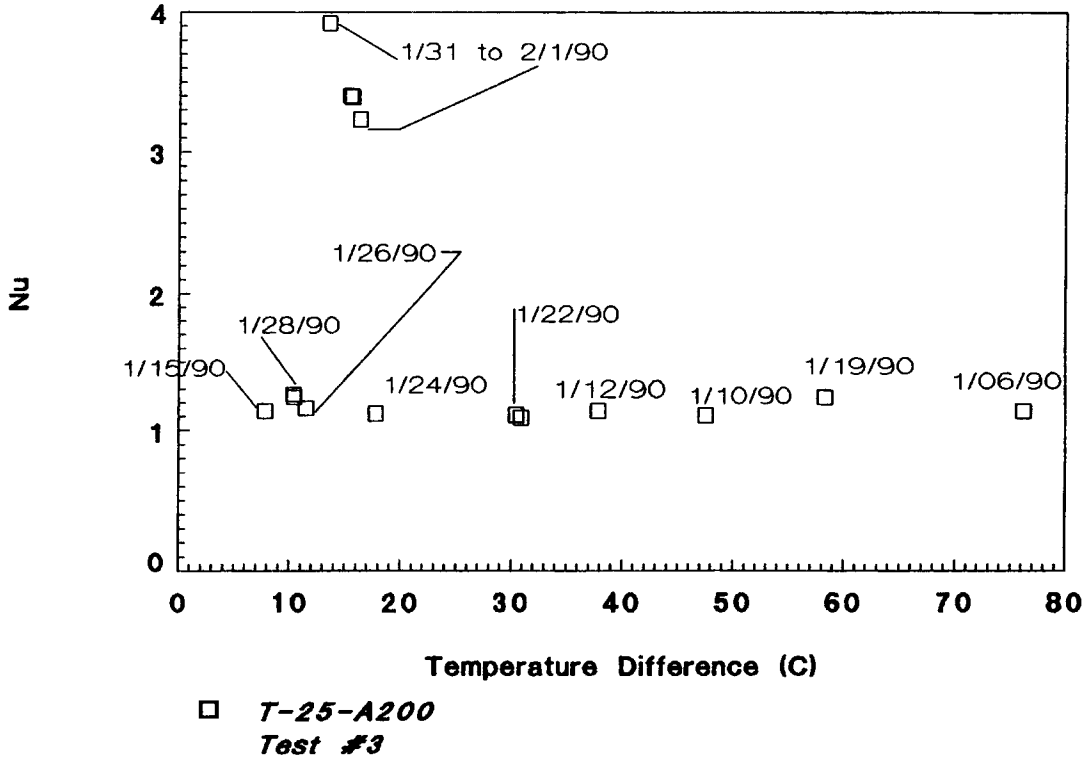

Figure 2 Nusselt number vs. temperature difference for a T-25-A200 HSPAN gel–water dispersion within 3 weeks of first heating.

separated by dashes as, for example, D–10–18–A200. The first identifier indicates whether the sample was mixed with distilled or tap water as denoted by a D or T, respectively. The second identifier indicates the ratio of HSPAN mass to water mass in units of hundredths of a percent (the second identifier for a 1% of HSPAN gel to water sample would be 100 while it would be 1 for a 0.01% of HSPAN material to water sample, for example). The third identifier is the Brookfield number of the spindle used. The fourth identifier denotes the HSPAN material. Thus, the example given above was with distilled water with 0.1% HSPAN material with a no. 18 spindle in the viscometer and A200 HSPAN material.

Because of the effects of velocity slip at both the rotating spindle and at the stationary beaker wall and of yield stress, as will be discussed later, the viscometer torque is not related to the spindle rotational speed in the conventional power-law manner. Nevertheless, plots of apparent viscosity vs. spindle rotational speed have utility in showing the effect of varying conditions on the viscous quality of the fluid. Unless otherwise noted, tests were performed at 20°C. The viscosity measurements for the A200 HSPAN material are representative of those for the other HSPAN materials, and many confirm the results reported by others. For the sake of brevity, only the results for the A200 HSPAN material are discussed in the next section.

A200 HSPAN Material

The viscosity measurements for the A200 HSPAN gel–water dispersions are reproducible, having only the typical scatter as the data for two sets of D–25–18–A200 new-material and D–25–18–A200 used-in-test-cell in Figure 3 show. Since the viscosity of water at room temperature is nearly equal to 1 cP, it is seen that these HSPAN gel–water dispersions can be as much as 20,000 times more viscous than water, a result that is consistent with that reported by Stannett et al.[3] and Gugliemelli et al.[7] A reduction in the apparent viscosity is seen to accompany a reduction in the HSPAN concentration as seen by the fact that the D–20–18–A200 new-material data are lower than the D–25–18–A200 new-material data. The D–25–18–A200 and D–25–18–A200 left-overnight-at-50°C data are similar, suggesting that a time of several hours at elevated temperature does not diminish apparent viscosity by much as previously reported by Gugliemelli et al.[7] The material listed as T–25–1–A200 from-top-of-test-cell was taken from the top of the convection test cell where it had remained at the temperature of the top cooling plate for the several week duration of convection test no. 3. This apparent viscosity was essentially unchanged from that of new material. Comparison of T–25–1–A200 from-top-of-test-cell data with D–25–18–A200 new-material data demonstrates that the effect of the impurities in the tap water is to reduce the viscous quality of the fluid. The T–50–1–A200 new-material data is comparable to the D–25–1–A200 new-material data suggesting that doubling the A200 HSPAN material concentration in tap water enables the same viscous quality to be obtained as with distilled water. The influence of heating for a period of about 4 weeks at about 50°C is seen for the T–25–18–A200 used-in-test-cell data for a sample taken from the bottom of the convection test cell. The apparent viscosity is about one-sixth that of new material represented by the T–25–18–A200 from-top-of-test-cell data. The appearance of the HSPAN gel–water dispersion after 4 weeks at elevated temperature in the convection test cell was thin and watery, in contrast to the thick and viscous appearance of the new material. The finding reported by Gugliemelli et al.[7] that apparent viscosity was little affected after 0.5 h at 100°C apparently did not hold true for times of the order of weeks at elevated temperature.

The effect of varying the A200 HSPAN material concentration is shown in Figure 3. Keeping in mind that the different spindles give different apparent viscosities for conditions that are otherwise identical, it is seen in Figure 3 that the apparent viscosity increases with increasing HSPAN material concentration. For example, the apparent viscosity of D–10–18–A200 new-material (0.1% HSPAN material concentration) is lower by a factor of about 20 than that of D–25–1–A200 new-material. That the apparent viscosity of D–10–18–A200 new-material is about 40 cP, and does not exhibit shear thinning might be due to the effect reported by Taylor and Bagley[17] that when gel particles are in low enough concentration to not be closely packed, the apparent viscosity is low and almost Newtonian.

Further tests were performed to ascertain the effect of elevated temperature on apparent viscosity. D–50–A200 HSPAN material was newly mixed; half was maintained at room temperature and half was heated for 3 days at 80°C in a beaker with a Saran Wrap cover to inhibit water loss by evaporation. Viscometer testing was done at room temperature for both samples. As shown in Figure 3, the apparent viscosity of the heated sample is about half that of the unheated sample. A greater decrease in apparent viscosity after 2 weeks at about 80°C in the con-

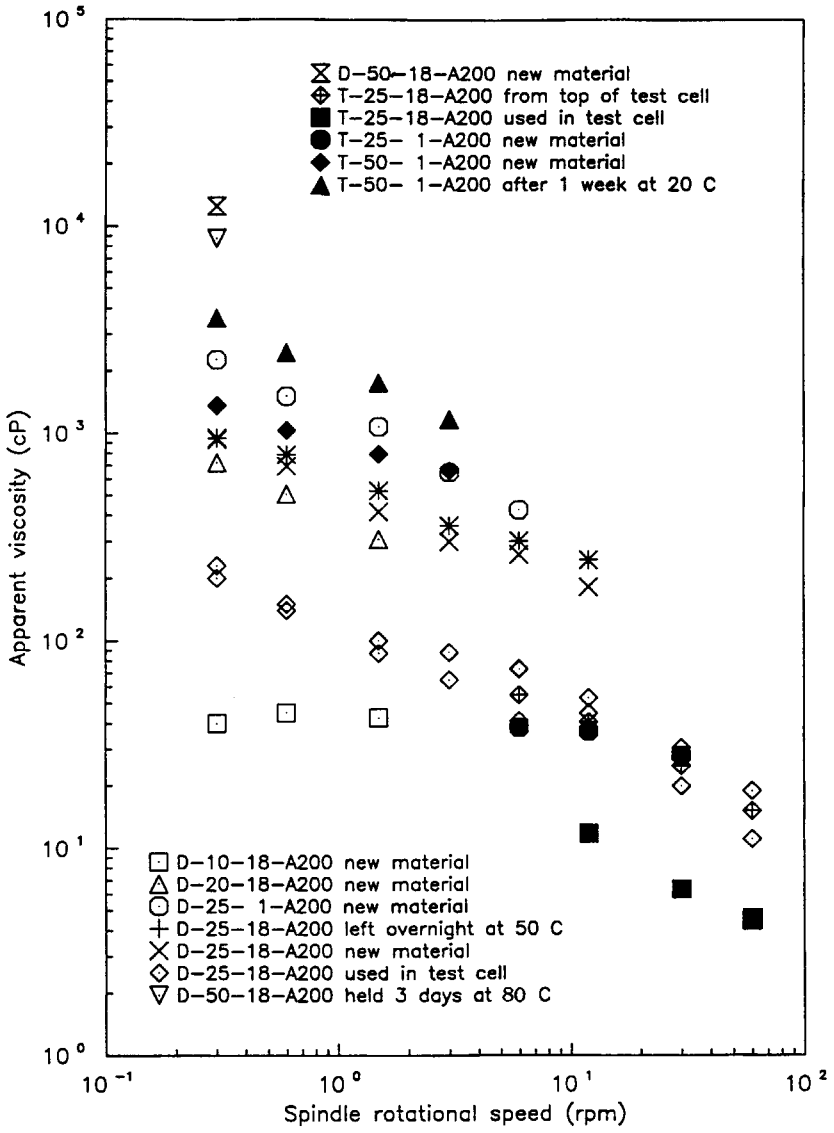

Figure 3 Apparent viscosity vs. spindle rotational speed for A200 HSPAN gel-water dispersions in tap and distilled water.

vection test cell is seen in Figure 3 since the D-25-18-A200 used-in-test-cell data is about one-sixth that of the D-25-18-A200 data for new material, consistent with the factor of six previously mentioned. The heat transfer coefficients measured in the convection test cell increased after 2 weeks of continuous use, testifying again to this change in the viscous properties of the HSPAN material-water dispersion. Apparent viscosity results are also shown in Figure 3 for T-25-A200 and T-50-A200. The T-50-1-A200 data show that setting at room temperature for 1 week produces an increase in apparent viscosity of about 30%. The T-25-18-A200 data for apparent viscosity after 2 weeks of continuous use in the convection test cell decreased by about a factor of 10 for the material taken from the top of the convection test cell where the temperature was near 30°C and by a factor of 40 for the material taken from the bottom of the convection test cell where the temperature was near 80°C.

YIELD STRESS AND VELOCITY SLIP

Examination of the motion of an HSPAN gel-water dispersion in the viscometer revealed behavior that had not been previously reported for this fluid. The fluid, before extended exposure to elevated temper-

ature, exhibits both a yield shear stress and velocity slip at solid surfaces. That an HSPAN gel–water dispersion has a yield shear stress was qualitatively mentioned by Taylor and Bagley.[4,18] Hydrolyzed cellulose polyacrylonitrile (HCPAN) material, made from cellulose rather than starch, was also qualitatively noted by Taylor and Bagley[17] to have a yield shear stress and later quantitatively reported by them.[19] Yield stresses were qualitatively reported by Bagley and Christianson[20] for wheat starch dispersions and by Christianson and Bagley[21] for corn starch dispersions, neither an HSPAN material. The phenomenon of slip discussed by Mooney,[22] Bird et al.,[23] and Luk et al.[24] can be mathematically treated as a discontinuity in velocity and has that appearance to the naked eye. Christianson and Bagley[21] mentioned the possibility of slip in a corn starch–water dispersion, but provided no measurement. Windhab et al.[25] reported yield stress values for gelatinized starch pastes, but only mentioned in a qualitative way that the effects of wall slip were taken into account.

The existence of these phenomena was made clear by drawing a radial ink line on the surface of the fluid in the beaker in which the viscometer spindle was centered before the spindle was set into rotation. After the spindle had rotated for several minutes the ink line showed, as in Figure 4(b), that the outer portion of the liquid rotated in plug flow, as a flywheel, slowly slipping past the stationary outer wall of the beaker. The inner core of liquid, where the shear stress exceeded the yield stress, flowed in a viscous manner with slip at the rotating spindle surface. The boundary between the inner viscous flow and the outer plug flow portions was readily apparent. The velocity slip at the solid boundaries might have been due to a thin layer of water there.

The relationships needed to conveniently identify the parameters that enable characterization of the viscous flow of the dispersion from rotating spindle viscometer data do not seem to have been worked out for the situation encountered in this study. Van Wazer et al.[9] worked them out for the case of a power law fluid with a yield stress, Fitch[26] did the same for a Newtonian fluid with a yield stress, and Mooney[22] did it for a Newtonian fluid with slip and spoke of the non-Newtonian case without explicit results. Those commonly used ones worked out by Krieger and Maron[27] and extended by Calderbak and Moo-Young[28] only apply to a fluid without slip. Accordingly, the development of the needed relationships follows.

TORQUE–ROTATIONAL SPEED RELATIONSHIPS

For a non-Newtonian fluid in the annulus between two very long concentric cylinders, the inner rotating one of radius r_i and the outer stationary one of radius r_o, the physical situation is as illustrated in Figure 4, where typical distributions of angular velocity ω

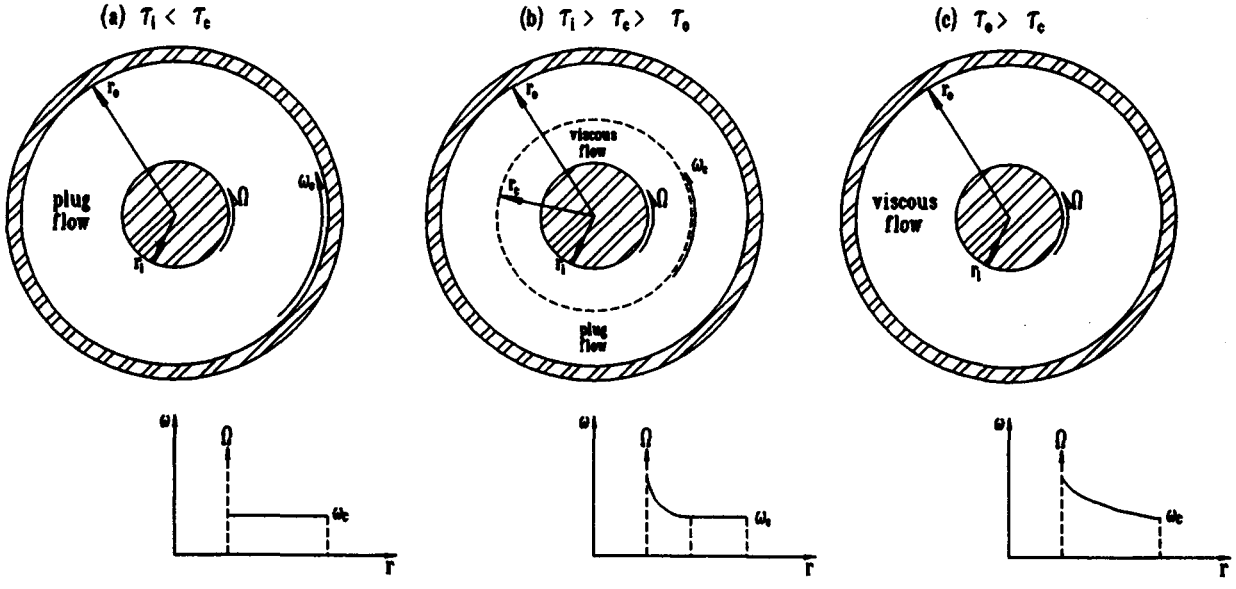

Figure 4 Couette flow regimes in the viscometer: (a) all plug flow; (b) both viscous and plug flow; (c) all viscous flow.

are shown with a yield stress τ_c occurring in the annulus. Slip velocities, $v_{s,i}$ at the inner cylinder and $v_{s,o}$ at the outer cylinder, are also shown. When the tangential shear stress τ_i at the inner cylinder is below the yield stress τ_c as in Figure 4(a), as would occur at low rotational speed Ω of the inner cylinder, the entire fluid rotates as a solid plug with constant angular velocity ω_c. At inner cylinder rotational speeds above a critical value Ω_1, the shear stress in the fluid exceeds the yield stress as in Figure 4(b) and the fluid near the cylinder undergoes viscous flow with plug flow occurring near the outer cylinder. At still higher inner cylinder rotational speeds above a second critical speed Ω_2, the yield stress is exceeded everywhere as in Figure 4(c) and viscous flow occurs everywhere. The inner cylinder represents the viscometer spindle and the outer cylinder represents the liquid container.

The yield shear stress can be evaluated by measuring the radius r_c, at which plug flow begins and viscous flow ceases, as illustrated in Figure 4(b). Since the tangential torque T must be constant at any radius r,

$$T = 2\pi L r^2 \tau$$

and shear stress τ must vary with radius as

$$\tau = \tau_i r_i^2 / r^2 \tag{1}$$

where τ_i is the shear stress at the inner cylinder. Here L is taken to be the actual spindle length, although, as discussed by Van Wazer et al.,[9] the effective length of a viscometer spindle is greater than the actual length. At the radius r_c the shear stress equals the yield stress and so, from eq. (1),

$$\tau_c = \tau_i r_i^2 / r_i^2 \tag{2}$$

Measurement of the radius of the interface between plug and viscous flow along with the viscometer torque enables the yield stress to be evaluated.

The velocity slip v_s is taken into account by the mathematical model suggested by Bird et al.[23]

$$v_s = B\tau \tag{3}$$

where B is the slip coefficient. At the outer cylinder,

$$v_{s,o} = r_o \omega_c \tag{4}$$

Use of eq. (1) in eq. (4) gives

$$B = r_o^3 \omega_c / \tau_i \tau_i^2 \tag{5}$$

Measurement of the angular velocity ω_c of the plug flow enables evaluation of the slip coefficient.

There will be no viscous flow until the shear stress τ_i at the inner cylinder exceeds the yield shear stress. Below the rotational speed Ω_1 of the cylinder at which this happens, the entire fluid in the annulus rotates as a solid body at the rotational speed ω_c. Application of eq. (3) at the inner cylinder, subject to the realization that there

$$v_{s,i} = (\Omega - \omega_c) r_i \tag{6}$$

gives

$$(\Omega - \omega_c) r_i = B\tau_i \tag{7}$$

Substitution of eq. (5) into eq. (7) to eliminate ω_c gives the linear variation of torque with inner cylinder rotational speed

$$\tau_i = (r_i \Omega / B) / (1 + r_i^3 / r_o^3), \quad \Omega < \Omega_1 \tag{8}$$

Equation (8) ceases to apply when the shear stress at the inner cylinder exceeds the yield stress, which occurs when $\Omega > \Omega_1$. Setting τ_i equal to τ_c in eq. (8) gives the limiting rotational speed of the inner cylinder as

$$\Omega_1 = B\tau_c (1 + r_i^3 / r_o^3) / r_i \tag{9}$$

Use of eq. (8) in eq. (5) to eliminate τ_i gives the rotational speed of the plug flow as

$$\omega_c = \Omega / (1 + r_o^3 / r_i^3), \quad \Omega < \Omega_1 \tag{10}$$

The viscous flow that occurs next to the inner cylinder when $\Omega > \Omega_1$ is described by the power-law model as

$$\tau = \tau_c - K |r\, d\omega/dr|^{-1+1/n} (r\, d\omega/dr), \quad \tau_c < \tau \tag{11}$$

in which ω is the rotational speed of the fluid in viscous flow and the coefficient K and exponent n are properties of the fluid. Noting that $d\omega/dr < 0$ and making use of eq. (1) enable eq. (11) to be rearranged as

$$-r\, d\omega/dr = (C/r^2 - 1)^n (\tau_c / K)^n \tag{12}$$

where

$$C = r_i^2 \tau_i / \tau_c$$

At the inner cylinder, according to eqs. (6) and (7),

$$r_i[\Omega - \omega(r_i)] = B\tau_i$$

from which the boundary condition

$$\omega(r_i) = \Omega - B\tau_i / r_i \qquad (13)$$

to be satisfied by eq. (11) is obtained. Another boundary condition for eq. (11) is obtained from the fact that, at the interface between viscous and plug flow regions where $r = r_c$,

$$\omega = \omega_c$$

After making use of eq. (5), this relationship is found to be

$$\omega(r_c) = (B\tau_i / r_i)(r_i / r_o)^3 \qquad (14)$$

Since n and K are to be determined from plots of torque vs. inner cylinder rotational speed, it is necessary to solve eqs. (12)–(14) to ascertain the manner in which the torque–rotational speed relationship depends upon K and n.

If n is an integer, the solutions to eqs. (12)–(14) are straightforward. The simplest case is for the Newtonian liquid ($n = 1$) for which integration of eq. (12) and application of the boundary conditions of eqs. (13) and (14) gives the nonlinear relationship

$$2K[\Omega - \tau_i B(1 + r_i^3/r_o^3)/r_i] = \tau_i - \tau_c + \tau_c \ln(\tau_i/\tau_c) \qquad (15)$$

in which eq. (2) has been employed. This differs from the result given by Fitch[26] only in that $B \neq 0$ here. For the power-law fluid for which $n = 2$, a similar procedure gives

$$4K^2[\Omega - \tau_i B(1 + r_i^3/r_o^3)/r_i] = (\tau_i - \tau_c)^2 - 2\tau_c(\tau_i - \tau_c) + 2\tau_c^2 \ln(\tau_i/\tau_c) \qquad (16)$$

It is seen that a logarithmic term appears and the series is finite when n takes on an integer value.

For noninteger values of n, the solution to eqs. (12)–(14) is an infinite series. When the shear stress in the viscous flow region only slightly exceeds the yield stress, $0 < \tau_i - \tau_c < \tau_c$, the transformation

$$z = (\tau - \tau_c)/\tau_c = Cr^{-2}/\tau_c - 1$$

puts eq. (12) into the form

$$2(K/\tau_c)^n \, d\omega/dz = z^n/(1 + z) \qquad (17)$$

Since $z < 1$, series expansion of the denominator of the right-hand side as

$$(1 + z)^{-1} = 1 - z + z^2 - z^3 + \cdots$$

followed by term-by-term integration and imposition of eqs. (13) and (14) gives

$$2(n + 1)\tau_c K^n[\Omega - \tau_i B(1 + r_i^3/r_o^3)/r_i] = (\tau_i - \tau_c)^{n+1} f(n, z_i)$$

where

$$z_i = \tau_i/\tau_c - 1$$

and

$$f(n, z_i) = 1 - (n + 1)z_i/(n + 2) + (n + 1)z_i^2/(n + 3) - (n + 1)z_i^3/(n + 4) \cdots$$

For $z_i \ll 1$, it is seen that

$$\tau_i - \tau_c = [2(n+1)\tau_c K^n(\Omega - \Omega_1 \tau/\tau_c)]^{1/(1+n)} \qquad (18)$$

Thus, the exponent n can be obtained from the slope of a log–log plot of $\tau_i - \tau_c$ vs. $\Omega - \Omega_1\tau_i/\tau_c$. Alternatively, τ_c can be obtained as the ordinate of a plot of τ_i vs.

$$[\Omega - \tau_i B(1 + r_i^3/r_o^3)/r_i]^{1/(1+n)}$$

if n and B are known. With τ_c and B already known and N obtained, the coefficient obtained from fitting a straight line through the data enables the parameter K to be evaluated. As pointed out by Fitch,[26] nonzero yield stresses result in nonlinear viscometer torque–spindle speed characteristics even for otherwise Newtonian fluids. This is also shown in eq. (18).

When the shear stress at the outer cylinder exceeds the yield stress, viscous flow occurs everywhere. Then similar procedures can be applied (see Hardin and Burmeister[29]) to obtain the critical speed Ω_2 above which that occurs as well as the relationship between the inner cylinder speed and the shear stress acting on it.

The case of $\Omega > \Omega_2$ did not occur for the measurements reported here.

Table I Slip Coefficients and Yield Stresses for HSPAN Gel–Water Dispersions

Sample	B (m^3/N s)	τ_c (N/m^2)	Ω (rev/min)
T-50-1-G400 ground	0.0251	1.549	12
T-50-1-G400	0.0185	2.424	30
T-25-1-G400	0.0208	0.917	0.6
T-25-1-G400	0.0403	1.438	1.5
D-25-1, 4-G400	0.0145	1.566	60
T-20-1-G400	0.0264	1.33	1.5
D-10-1-G400	0.3502	0.04	6
T-50-1-A200	0.0481	0.36	3
D-40-1-A200	0.216		60
D-30-1-A200	0.0223	0.357	0.6
D-30-1-A200	0.124		12
D-25-1-A200	0.0609	0.16	30

YIELD STRESS AND SLIP COEFFICIENT MEASUREMENTS

Measurements of the slip coefficient B and the yield stress τ_c were made for the A200 and G400 Water Lock HSPAN materials with similar results as shown in Table I. Equations (2) and (5) were used to relate the measured viscometer torque T and corresponding shear stress τ_i at the viscometer spindle, critical radius r_c to the interface between viscous and plug flow regions, and rotational speed ω_c of the plug flow region to the slip coefficient B and the yield stress τ_c. Cylindrical Brookfield spindles nos. 1 and 4 were exclusively used. The slip coefficient is often, but not always, higher for HSPAN material dispersed in distilled water than in tap water by about an order of magnitude. The yield stress was not much affected by the difference between tap and distilled water, however.

To determine the effect of dry HSPAN particle size, one sample of the G400 HSPAN material was ground into a powder in a mortar with a pestle. A powdered dispersion in the same tap water and at the same mass ratio as an as-received sample gave a 35% increase in slip coefficient and a 36% reduction in yield stress. The particle size of the dry HSPAN material affected these two parameters values somewhat.

Some of the variations in the values shown in Table I are believed to be due to the influence of

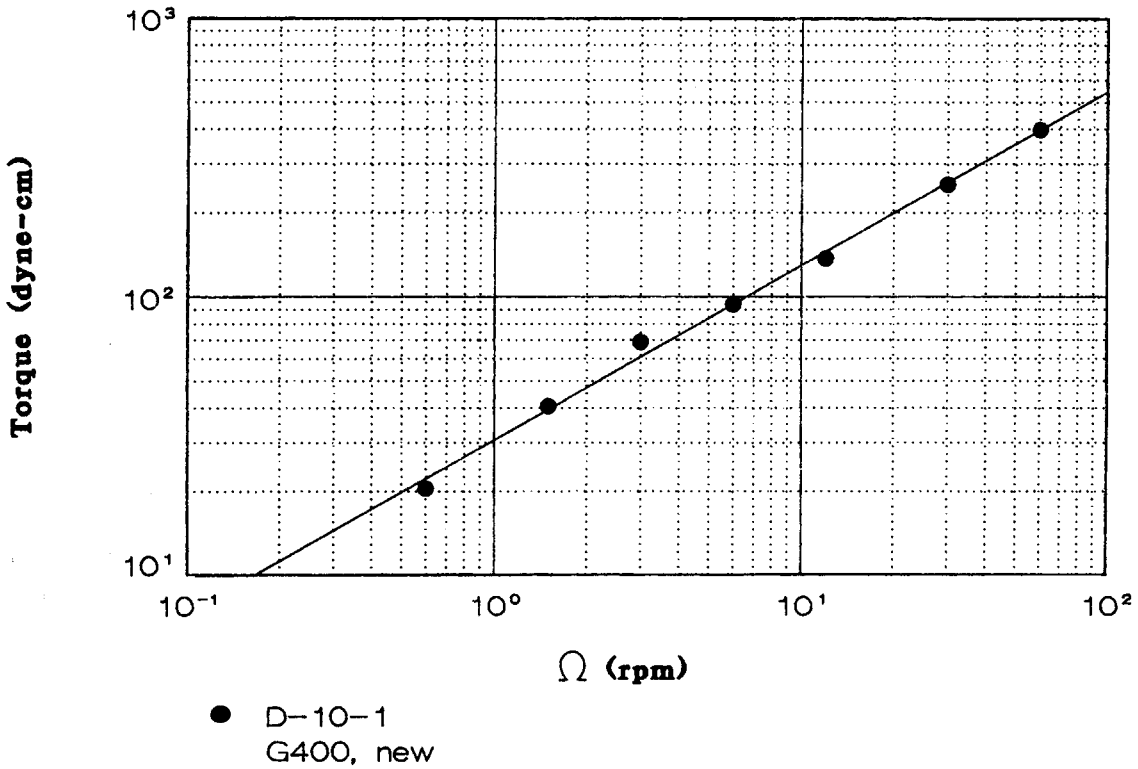

Figure 5 Viscometer torque vs. spindle rotational speed for a D-10-1-G400 HSPAN gel–water dispersion.

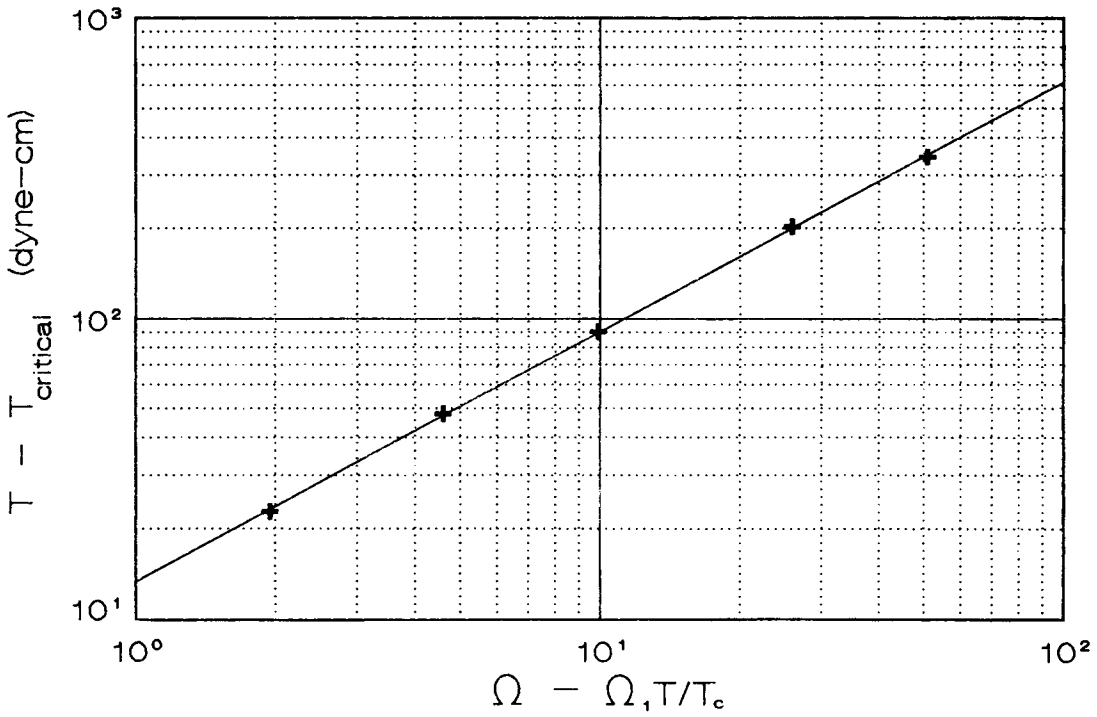

Figure 6 Net viscometer torque vs. net spindle rotational speed for a D-10-1-G400 HSPAN gel–water dispersion.

spindle speed. Comparison of the two results for T-25-1-G400 samples at different spindle speeds shows different parameter values, for example. Thus the foregoing comments are tentative since spindle speed often differed between the cases in Table I.

The accuracy of these slip and yield stress measurements can be judged by the goodness with which a plot of viscometer torque vs. spindle rotational speed can be fitted and the constants of the describing equation determined. Such measurements for the G400 HSPAN material are shown in Figure 5, where it is seen that viscometer torque varies with spindle rotational speed in a manner that is suggestive of power-law behavior, although a straight line does not fit the data perfectly. The same data are plotted in Figure 6 in accordance with the suggestion of eq. (18), $\tau - \tau_i$ vs. $\Omega - \Omega_i \tau_i / \tau_c$, and are seen to be almost perfectly fitted with a straight line if the yield stress value is taken to be half that given in Table I but with the slip coefficient value cited there. The parameter values for eq. (18) were tentatively found to be $n = 0.207$ and $K = 0.063\ N\ s^{4.83}/m^2\ rad^{4.83}$. The flow behavior of this G400 HSPAN gel–water dispersion seems to be characterized as that of a power-law fluid with a yield stress and a velocity slip coefficient. Yield stress and slip coefficient determinations were not made for the other HSPAN gel–water dispersions. Greater detail of method and result is reported by Hardin and Burmeister.[29]

CONCLUSIONS

An HSPAN gel–water dispersion can possess the characteristics of velocity slip at solid boundaries and a yield stress. The yield stress enables an HSPAN gel–water dispersion fluid to withstand greater temperature differences across a horizontal layer than a fluid, such as water, without one. The fluid with HSPAN concentrations of 0.25% concentration was about 10,000 times more viscous than water when the shear stress surpassed the yield stress and viscous power-law flow ensued. The apparent viscosity of an HSPAN material–water dispersion was reduced by nearly an order of magnitude when tap water was substituted for distilled water as the solvent, decreased by about 30% after the fluid was continuously maintained at a temperature of 80°C for 1 week, and by about an order of magnitude after 3 weeks under those conditions.

APPENDIX: NOMENCLATURE

A_c temporary cover area (m^2)
B slip coefficient ($m^3/N\ s$)
C constant
f function (dimensionless)
G function (dimensionless)
g gravitational acceleration (m/s^2)
h heat transfer coefficient ($W/m^2\ K$)
K power-law coefficient ($N\ s^{1/n}/m^2$)
KL loss coefficient for convection cell sides and bottom ($W/°C$)
k styrofoam thermal conductivity ($W/m\ °C$)
L horizontal fluid layer thickness, cylinder length (m)
n power-law exponent (dimensionless)
Nu Nusselt number, $Nu = hL/k$ (dimensionless)
r radius (m)
r_c radius at which plug flow begins (m)
QL heat loss from the convection cell sides and bottom (W)
QLC heat loss through temporary styrofoam cover (W)
Ra Rayleigh number, $Ra = g\beta\Delta TL^3/\nu\alpha$ (dimensionless)
T torque ($N\ m$); temperature (°C)
T_{av} average temperature in the convection cell (°C)
T_{bo} temperature of the heating plate upper side (°C)
T_r room temperature (°C)
T_{top} temperature of the cooling plate under side (°C)
T_{uh} temperature of the heater under side (°C)
ΔT temperature difference between the fluid layer top and bottom (°C)
v_s slip velocity (m/s)
z shear stress ratio, $z = (\tau - \tau_c)/\tau_c$ (dimensionless)

Greek Symbols

α fluid thermal diffusivity (m^2/s)
β fluid coefficient of thermal expansion ($°C^{-1}$)
$\dot{\gamma}$ shearing rate (s^{-1})
μ apparent viscosity ($N\ s/m^2$)
μ_0 zero-shear rate viscosity for modified power-law ($N\ s/m^2$)
ν fluid kinematic viscosity (m^2/s)
τ shear stress (N/m^2)
τ_c yield shear stress (N/m^2)
ω angular speed (rad/s)
ω_c plug angular speed (rad/s)
Ω inner cylinder angular speed (rad/s)
Ω_1 angular speed below which all is plug flow (rad/s)
Ω_2 angular speed above which all is viscous flow (rad/s)

Subscripts

i evaluated at the inner cylinder
o evaluated at the outer cylinder

The sponsorship of the Kansas Corn Commission for this study is gratefully acknowledged. The senior author held a Carey Fellowship through the Department of Mechanical Engineering as well.

REFERENCES

1. M. O. Weaver, R. R. Montgomery, L. D. Miller, V. E. Sohns, G. F. Fanta, and W. F. Doane, *Staerke,* **29,** 413 (1977).
2. F. H. Otey and W. M. Doane, *Starch: Chemistry and Technology,* 2nd ed., R. L. Whistler, J. N. Bemiller, and E. F. Paschall, Eds., 1984, p. 406.
3. V. T. Stannett, W. M. Doane, and G. F. Fanta, *Absorbency,* P. K. Chatterjee, Ed., Elsevier, New York, 1985, p. 257.
4. N. W. Taylor and E. B. Bagley, *J. Appl. Polym. Sci.,* **18,** 2747 (1974).
5. N. W. Taylor and E. B. Bagley, *J. Appl. Polym. Sci.,* **21,** 113 (1977).
6. E. B. Bagley and N. W. Taylor, *Ind. Eng. Chem. Prod. Res. Dev.,* **14,** 105 (1975).
7. L. A. Gugliemelli, M. O. Weaver, C. R. Russell, and C. E. Rist, *J. Appl. Polym. Sci.,* **13,** 2007 (1969).
8. M. O. Weaver, L. A. Gugliemelli, W. M. Doane, and C. R. Russell, *J. Appl. Polym. Sci.,* **15,** 3015 (1971).
9. J. R. Van Wazer, J. W. Layons, K. Y. Kim, and R. E. Colwell, *Viscosity and Flow Measurement,* Wiley-Interscience, New York, 1963.
10. A. V. Shenoy, *Handbook of Heat and Mass Transfer,* N. P. Cheremisinoff, Ed., Gulf Publishing Co., Houston, TX, 1986, Vol. 1, p. 195.
11. I. Catton, *Trans. ASME J. Heat Transfer,* **92,** 186 (1970).
12. I. Catton, *Trans. ASME J. Heat Transfer,* **94,** 446 (1972).
13. I. Catton, *Int. J. Heat Mass Transfer,* **15,** 665 (1972).
14. S. W. Churchill, *Heat Exchanger Design Handbook,* Hemisphere, New York, 1986, Vol. 2, p. 2.5.8-1.
15. K. G. T. Hollands, S. E. Unny, G. D. Raithby, and L. Konicek, *J. Heat Transfer,* **98,** 189 (1976).
16. T. Makino, M. Maerefat, and R. Kunitomo, *Solar En-*

ergy—1987, Proc. ASME-JSME Solar Energy Conf., Honolulu, Hawaii, March 22–27, ASME, New York, 1987, Vol. 1, p. 172.
17. N. W. Taylor and E. B. Bagley, *J. Appl. Polym. Sci.*, **21,** 1607 (1977).
18. E. B. Bagley and N. W. Taylor, *J. Polym. Sci. Polym. Symp.*, **45,** 185 (1974).
19. N. W. Taylor and E. B. Bagley, *J. Appl. Polym. Sci.*, **23,** 1897 (1979).
20. E. B. Bagley and D. D. Christianson, *Staerke,* **35,** 81 (1983).
21. D. D. Christianson and E. B. Bagley, *Cereal Chem.*, **61,** 500 (1984).
22. M. Mooney, *J. Rheol.*, **2,** 210 (1932).
23. R. B. Bird, R. C. Armstrong, and O. Hassager, *Dynamics of Polymeric Liquids,* 2nd ed., Wiley-Interscience, New York, 1987, Vol. 1, p. 247.
24. S. Luk, R. Mutharasan, and D. Apelian, *Ind. Eng. Chem. Res.*, **26,** 1609 (1987).
25. E. Windhab, G. Tegge, and U. Tiemeier, *Staerke,* **40,** 20 (1988).
26. E. B. Fitch, *Ind. Eng. Chem.*, **51,** 889 (1959).
27. I. M. Krieger and S. H. Maron, *J. Appl. Phys.*, **25,** 72 (1954).
28. P. H. Calderbank and M. B. Moo-Young, *Trans. Inst. Chem. Eng. (Lond.),* **37,** 26 (1959).
29. R. Hardin and L. Burmeister, in Proc. 28th National Heat Transfer Conference, July 28–31, 1991, Minneapolis, MN, HTD, Vol. 174, ASME, New York, 1991.

Received October 7, 1991
Accepted July 24, 1992